Computers and Structures 90–91 (2012) 55–64

Contents lists available at SciVerse ScienceDirect

Computers and Structures

journal homepage: www.elsevier.com/locate/compstruc

A level set solution to the stress-based structural shape and topology optimization

Qi Xia [a], Tielin Shi [a], Shiyuan Liu [a], Michael Yu Wang [b,*]

[a] The State Key Laboratory of Digital Manufacturing Equipment and Technology, Huazhong University of Science and Technology, Wuhan, China
[b] Department of Mechanical and Automation Engineering, The Chinese University of Hong Kong, Shatin, NT, Hong Kong

ARTICLE INFO

Article history:
Received 31 May 2011
Accepted 10 October 2011
Available online 5 November 2011

Keywords:
Shape and topology optimization
Level set method
Stress

ABSTRACT

We present a level set solution to the stress-based structural shape and topology optimization. First, a novel global measure of stress is proposed, and the optimization problem is formulated to minimize the global measure of stress subject to a constraint of material volume. In order to solve this optimization problem, the level set method is employed. The finite element analysis is accomplished by modifying a fixed background mesh, and the artificial weak material that is conventionally used in the level set method to mimic void is avoided in the present work.

1. Introduction

Stress is a significant design criterion in practical engineering applications. The stress-based shape and topology optimization is a challenging problem and has been extensively studied during the past decades.

Zienkiewicz and Campbell [1] pioneered to apply finite element method to shape optimization, and Francavilla et al. [2] applied the shape optimization to minimize stress concentration. Various stress-based functions for shape optimization, such as the maximum von Mises stress and stress leveling, were proposed. Readers are referred to [3,4] and the references therein for a review of the stress-based shape optimization.

Since the seminal work of the homogenization based method by Bendsøe and Kikuchi [5] and the SIMP (solid isotropic microstructure with penalization) method by Bendsøe [6], structural topology optimization has become an effective tool for obtaining efficient structures, and much effort has been made for the stress based topology optimization. Yang and Chen [7] proposed a weighted combination of compliance and p-norm of stress as the objective function. A topology optimization problem that takes local stresses as constraints was proposed by Duysinx and Bendsøe [8] and was solved by the SIMP method. Allaire et al. [9] employed the homogenization method to minimize a global measure of stress of structures constituted by sequential laminated composites. Using the SIMP method, Pereira et al. [10] studied the topology optimization with material failure constraints. Bruggi and Venini [11] proposed to use a mixed finite element method to compute the stress for the stress-constrained topology optimization, which is more accurate than displacement-based finite element methods. Also using the SIMP method, París et al. [12,13] studied the weight minimization problems with global or local stress constraints, in which the global stress constraints are defined by the Kreisselmeier–Steinhauser function. Le et al. [14] employed the SIMP method, a SIMP-motivated stress definition, p-norm, normalized global stress measure, and regional stress measure to solve the stress-constrained topology optimization.

Svanberg and Werme [15] applied the linear mixed 0–1 model and sequential integer programming method for the stress constrained topology optimization. Li et al. [16] studied the ESO (evolutionary structural optimization) method for stressed minimization. Amstutz and Novotny [17] studied the topological derivative method for the topology optimization with a stress-based objective function constructed by combination of material volume, compliance, and the p-norm of von Mises stress. A level set based method is proposed by Allaire and Jouve [18] to minimize a domain integral of stress subject to material volume constraint. Using X-FEM and level set, Miegroet and Duysinx [19] studied the shape optimization for minimizing stress concentration.

The stress-based shape and topology optimization problems are challenging because there exist much numerical difficulties in solving such problems. The major reason of such difficulties lies in the fact that the stress is a local identity. In other word, the stress at each point in a continuum structure should be ensured to be smaller than an admissible stress. However, when local stresses are treated as constraints in the optimization, there will be a big number of constraints, and the computational costs of sensitivity analysis of such constraints, whether it is treated by the direct method or the adjoint method, will be huge. Therefore, a constraint selection strategy was proposed by Duysinx and Bendsøe [8]. As the result, only the potentially active stress constraints are considered during the optimization, thus saving the computational costs

* Corresponding author. Tel.: +852 2609 8487; fax: +852 2603 6002.
E-mail address: yuwang@mae.cuhk.edu.hk (M.Y. Wang).

0045-7949/$ - see front matter © 2011 Elsevier Ltd. All rights reserved.
doi:10.1016/j.compstruc.2011.10.009

for sensitivity analysis of inactive constraints. Another effective way to reduce the computational costs is to use a global measures of stress in the stress-based topology optimization. However, although a global approach alleviates the computational costs, it turns out to be difficult to control peak stress or stress concentration. To deal with this difficulty, people employed the p-norm, p-mean, and Kreisselmeier–Steinhauser (K–S) function as the global measure. Generally, big p is taken for the p-norm or p-mean, or big penalty parameter is taken for the K–S function [7,12], to make the peak stress play a prominent role during the course of optimization. In such cases, however, convergence oscillation and numerical overflow may arise [20].

In view of the above-mentioned numerical difficulties, we define a novel global measure of stress in the present study. One part of the global measure is an integral of a power function of the von Mises stress, and the other part is a penalty of the von Mises stress that is bigger than a prescribed threshold. The optimization problem is formulated to minimize the global measure of stress subject to a constraint of material volume, and the level set based method [21–25] is employed to solve the optimization problem.

Conventionally, in the level set based method an Eulerian method employing a fixed mesh and ersatz material is used for the finite element analysis (FEA). According to this method, instead of performing FEA for the structure Ω, one performs FEA on a reference domain D that includes the structure, i.e., $\Omega \subset D$, with the void $D\backslash\overline{\Omega}$ being mimicked by an artificial weak material. However, this approach of FEA is not accurate enough for the stress-based topology optimization and gives rise to several delicate numerical issues that are described as follows.

Let us consider two structures that have the same geometry, the same boundary conditions, and the same loading conditions, but different Young's modulus of the material, for instance E and $E \cdot 10^{-3}$. It can be readily found out that the stresses are exactly the same in the two structures. Therefore, if one uses artificial weak material to mimic void but defines the global measure of stress only for solid material, there may be a trivial solution of the optimization problem, i.e., the reference domain filled with the artificial weak material. This phenomenon was also described in Ref. [14]. On the other hand, if one defines the global measure of stress for both solid and artificial weak material, one needs to redefine the stress for the artificial weak material. For example, under the same strain, redefine the stress of the artificial weak material to be bigger than that of the solid material. However, this will be a delicate numerical issue. Therefore, in the present study, we choose to eliminate the artificial weak material in the FEA.

Employing the level set based method and eliminating the artificial weak material has another benefit for the stress-based topology optimization, which is concerned with a well-known numerical difficulty called the "singularity phenomenon" [26–29]. The singularity phenomenon will arise when stresses are modeled as design-depended constraints [29] in a topology optimization problem. For instance, a stress constraint is design-depended in the SIMP model, since it is valid only when the design variable, i.e., the relative density, is nonzero (means that material exists at that point) and should be eliminated from the optimization problem when the relative density is zero or is at its lower bound (means that material dose not exist at that point). The consequence of the singularity phenomenon is that the optimal solution becomes a singular point in the design space, and that standard gradient based optimization algorithms are unable to reach the singular point [26–29]. The reason of the singularity phenomenon lies in the discontinuity of the admissible stress σ_a when the design variable, for instance the relative density ρ in the SIMP method, approaches zero [27]. In fact, σ_a should be positive infinity for $\rho = 0$, but should be bounded for $\rho > 0$. In order to deal with the singularity phenomenon, ε-relaxation method [30] or its variants [14,31] are often used. The key idea of these methods is to artificially define an admissible stress as a continuous function of the design variable. One can see that the singularity phenomenon is not due to the stress itself but due to the mathematical model of the topology optimization problem. In other word, if stress constraints are not modeled as design-dependent, the singularity phenomenon will not arise. We can see that when the stress-based topology optimization is model by the level set based method, the stress will not be design-dependent.

In view of the above-mentioned reasons, we take the level set based method and a strict 0–1 model (i.e., there is no artificial weak material that is conventionally used in the level set based method to mimic void) for the stress-based topology optimization. The paper is organized as follows. In Section 2 formulation of the topology optimization problem is described. In Section 3 sensitivity analysis for the optimization problem is described. In Section 4 the level set method is briefly described, and issues related to its application in topology optimization are discussed. Section 5 describes the finite element analysis. Section 6 gives numerical examples and discussions. Section 7 concludes this paper.

2. Stress minimization problem

A shape $\Omega \subset \mathbb{R}^d$ ($d = 2$ or 3) is an open bounded set occupied by isotropic linear elastic solid material. The Lipschitz continuous boundary of Ω consists of three disjoint parts

$$\partial\Omega = \Gamma_D \cup \Gamma_N \cup \Gamma_H$$

where a Dirichlet boundary condition is imposed on Γ_D, a Neumann boundary condition on Γ_N, and a homogeneous Neumann boundary condition, i.e., traction free, on Γ_H. In the present study, Γ_H is the only part subject to optimization and is free to move during the course of optimization.

The displacement field u in Ω is the unique solution of the linear elasticity system

$$\begin{cases} -\text{div } \sigma(u) = f & \text{in } \Omega \\ u = 0 & \text{on } \Gamma_D \\ \sigma(u)n = t & \text{on } \Gamma_N \end{cases} \tag{1}$$

where $\sigma(u) = Ae(u)$ is the stress tensor; A describes the Hooke's law; $e(u)$ is the strain tensor; f is the body force; t is the boundary traction force; n is the unit outward normal to the boundary.

The weak form of the linear elasticity system Eq. (1) is given by

$$a(u, v) = \ell(v), \quad \forall\ v \in U \tag{2}$$

where $U = \{v \in H^1(\Omega)^d | v = 0 \text{ on } \Gamma_D\}$ is the space of kinematically admissible displacement fields, and $a(u, v)$ and $\ell(v)$ are defined as

$$\begin{aligned} a(u, v) &= \int_\Omega Ae(u) \cdot e(v)\mathrm{d}x \\ \ell(v) &= \int_\Omega f v\mathrm{d}x + \int_{\Gamma_N} g v\mathrm{d}s \end{aligned} \tag{3}$$

The optimization problem of the present work is to minimize a global measure of von Mises stress subject to a constraint of material volume, which is given by

$$\begin{aligned} &\min\ J = \textstyle\int_\Omega g(\sigma_v)(\alpha_1 + \alpha_2 H(\sigma_v - \bar{\sigma}))\mathrm{d}x \\ &\text{s.t. } a(u, v) = \ell(u, v), \forall v \in U \\ &\quad V - \overline{V} \leqslant 0 \end{aligned} \tag{4}$$

where $V = \int_\Omega \mathrm{d}x$ is the volume of structure, and $\overline{V}$ is the limit of volume.

The function g in the objective function can be any monotonically increasing function, and in the present study we employ the power function given by

$$g(\sigma_v) = \sigma_v^p \tag{5}$$

where p is a positive integer and is a parameter specified before the optimization. σ_v is the von Mises stress, and in 2D it is given by

$$\sigma_v = \sqrt{\sigma_{xx}^2 + \sigma_{yy}^2 - \sigma_{xx}\sigma_{yy} + 3\sigma_{xy}^2} \tag{6}$$

The function H in the objective function is the Heaviside function, and in practical numerical implementation it is usually approximated by continuous functions. In the present study, the approximate Heaviside function is defined as

$$H(x) = \begin{cases} 0, & x < -\Delta \\ \frac{3}{4}\left(\frac{x}{\Delta} - \frac{x^3}{3\Delta^3}\right) + \frac{1}{2}, & -\Delta \leqslant x < \Delta \\ 1, & x \geqslant \Delta \end{cases} \tag{7}$$

The derivative of the Heaviside function is the Dirac function that is given by

$$\delta(x) = \begin{cases} \frac{3}{4\Delta}\left(1 - \frac{x^2}{\Delta^2}\right), & |x| \leqslant \Delta \\ 0, & |x| > \Delta \end{cases} \tag{8}$$

It can be seen that the approximate Heaviside function is differentiable, and its derivative is continuous, i.e., $H \in C^1$. The $\overline{\sigma}$ in the objective function is a parameter specified before optimization. In fact, it is a threshold of von Mises stress above which the stress is penalized, and the parameters α_1 and α_2 control the weight of penalization. This penalization is very important for controlling peak stress in the stress-based shape and topology optimization since it makes peak stress play a prominent role during the course of optimization. Fig. 1 shows the plots of the approximate Heaviside function $H(\sigma_v - \bar{\sigma})$ and the approximate Dirac function $\delta(\sigma_v - \bar{\sigma})$ with $\bar{\sigma} = 20$ and different value of Δ. From Fig. 1, one can see that when Δ increases, the band of transition becomes wider and smoother.

3. Sensitivity analysis

In order to solve the optimization problem via a gradient based method, with the free boundary of a shape constituting the design variable, it is required to find the effect of boundary shape variation on the variations of functions. In this section we describe the sensitivity analysis for the stress minimization problem. The material derivative [32,33] and the adjoint method are employed.

The Lagrangian is defined as

$$\mathscr{L} = J + a(u, w) - \ell(w) + \lambda\left(\int_\Omega \mathrm{d}x - \overline{V}\right) \tag{9}$$

where $w \in U$ is a Lagrange multiplier for the equation of linear elasticity system Eq. (2), λ is a Lagrange multiplier for the constraint of material volume.

The material derivative of the Lagrangian is given by

$$\mathscr{L}' = J' + a'(u, w) - \ell'(w) + \lambda \int_\Omega V_n \mathrm{d}s \tag{10}$$

where the material derivatives J' is given by

$$\begin{aligned} J' = &\int_\Omega g'(\sigma_v)(\alpha_1 + \alpha_2 H(\sigma_v - \bar{\sigma}))\mathrm{d}x + \int_\Omega \alpha_2 g(\sigma_v) H'(\sigma_v - \bar{\sigma})\mathrm{d}x \\ &+ \int_{\partial\Omega} g(\sigma_v)(\alpha_1 + \alpha_2 H(\sigma_v - \bar{\sigma}))V_n \mathrm{d}s \end{aligned} \tag{11}$$

where the derivative g' and H' are given by

$$\begin{aligned} g'(\sigma_v) &= \frac{\partial g}{\partial \sigma_v}\frac{\partial \sigma_v}{\partial \sigma_{ij}}\sigma_{ij}(u') \\ H'(\sigma_v - \bar{\sigma}) &= \delta(\sigma_v - \bar{\sigma})\frac{\partial \sigma_v}{\partial \sigma_{ij}}\sigma_{ij}(u') \end{aligned} \tag{12}$$

where

$$\frac{\partial \sigma_v}{\partial \sigma_{ij}}\sigma_{ij}(u') = \frac{1}{2\sigma_v}[2\sigma_{xx} - \sigma_{yy}, 2\sigma_{yy} - \sigma_{xx}, 6\sigma_{xy}]\sigma(u') \tag{13}$$

The derivative $a'(u,w)$ and $\ell'(w)$ are given by

$$a'(u,w) = \int_\Omega Ae(u')\cdot e(w)\mathrm{d}x + \int_\Omega Ae(u)\cdot e(w')\mathrm{d}x + \int_{\partial\Omega} Ae(u)\cdot e(w)V_n \mathrm{d}s \tag{14}$$

$$\ell'(w) = \int_\Omega fw'\mathrm{d}x + \int_{\partial\Omega} fwV_n \mathrm{d}s + \int_{\Gamma_N} tw'\mathrm{d}s + \int_{\Gamma_N} (\nabla(tw)^T n + \kappa tw)V_n \mathrm{d}s \tag{15}$$

Substitute Eqs. (11)–(15) into Eq. (10), we obtain the material derivative of the Lagrangian. Collecting all the terms that contain w' in $\mathscr{L}'$ and letting the sum of these terms to be zero, we recover the weak form of the state equation, that is

$$\int_\Omega Ae(u)\cdot e(w')\mathrm{d}x = \int_\Omega fw'\mathrm{d}x + \int_{\Gamma_N} tw'\mathrm{d}s, \quad \forall w' \in U$$

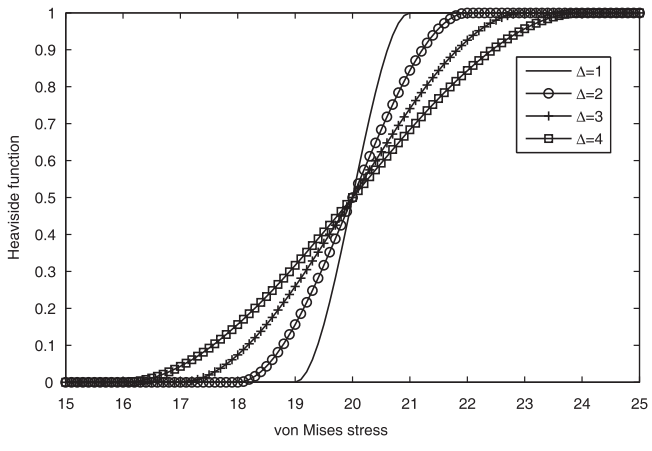

(a) $H(\sigma_v - \overline{\sigma})$

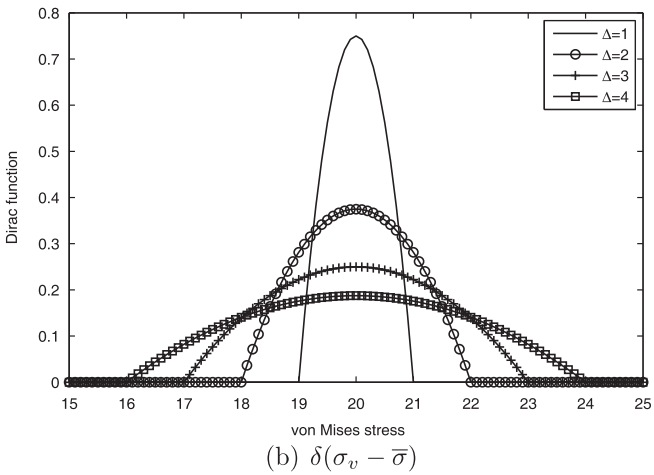

(b) $\delta(\sigma_v - \overline{\sigma})$

Fig. 1. The approximate Heaviside function and Dirac function with $\bar{\sigma} = 20$.

Collecting all the terms that contain u', and letting the sum of these terms to be zero, we obtain the adjoint equation, that is

$$\int_\Omega Ae(u')\cdot e(w)\mathrm{d}x = -\int_\Omega \left(\frac{\partial g}{\partial \sigma_v}(\alpha_1+\alpha_2 H(\sigma_v-\bar{\sigma})) + \alpha_2 g(\sigma_v)\delta(\sigma_v-\bar{\sigma})\right)\frac{\partial \sigma_v}{\partial \sigma_{ij}}\sigma_{ij}(u')\mathrm{d}x, \quad \forall u'\in U \tag{16}$$

Finally, collecting all the terms that contain V_n, assuming there exists no body force, i.e., $f = 0$, and noticing that only Γ_H subjects to optimization, we obtain the shape derivative of the Lagrangian

$$\mathscr{L}' = \int_{\Gamma_H} GV_n\mathrm{d}s, \quad G = g(\sigma_v)(\alpha_1+\alpha_2 H(\sigma_v-\bar{\sigma})) + Ae(u)\cdot e(w) + \lambda \tag{17}$$

where G is called the shape gradient density.

During optimization, the Lagrange multiplier λ is updated according to the augmented Lagrange multiplier method by

$$\lambda^{k+1} = \max\left\{0, \lambda^k + \frac{1}{\mu}(V^k - \overline{V})\right\} \tag{18}$$

The benefit of augmented Lagrangian multiplier method is that the Lagrangian multiplier can be iteratively updated so that one can obtain a reasonable estimate of exact Lagrange multiplier [34]. In other words, the volume of material of the structure can be driven to be very close to that prescribed in the problem formulation even when μ is not sufficiently close to zero.

According to Eq. (17), we can readily obtain a descent direction for the optimization problem. In the simplest form, it amounts to choose the steepest descent direction, which can be obtained by setting

$$V_n(x) = -G(x), \quad \forall x\in\Gamma_H \tag{19}$$

It can be seen that such V_n will yield $\mathscr{L}' = -\int_{\Gamma_H} G^2\mathrm{d}s \leqslant 0$ which implies the descent of the Lagrangian.

However, it is well known that the steepest descent method is not so efficient in the family of optimization algorithms. In order to speed up the convergence of the optimization, a conjugate mapping [35,36] of the velocity V_n is used in the present work. First, V_n is normalized by the maximum value of $|V_n|$, then a mapping given in the following is applied.

$$F(x) = xe^{(1-|x|)} \tag{20}$$

The key idea of the conjugate mapping is to increase the difference of the velocity along the free boundary while keeping the objective function to descent. This is particularly useful in the stress-based topology optimization since there may exist peak stress, and the velocity at the point of peak stress may be much bigger than that at the other points on the free boundary.

4. The level set method

Level set is a method to represent and track moving boundary, and more importantly, it is transparent to topological changes, which is significant for topology optimization. With such transparent treatment of topological change the difficult topology optimization problem can be transformed to a relatively easier shape optimization problem. The level set method was first introduced to structural shape and topology optimization by Sethian and Wiegmann [21], and it has caught much attention since the seminal papers [22–25].

The boundary of a shape Ω is nonintersecting, Lipschitz-continuous and represented implicitly through a Lipschitz-continuous level set function $\Phi(x)$ as its zero isosurface or zero level set, i.e., $\{x\in\mathbb{R}^d|\Phi(x)=0\}$ ($d = 2$ or 3), and $\Phi(x)$ can be used to define the inside and outside regions with respect to the boundary as follows

$$\begin{aligned}&\Phi(x) = 0 \Longleftrightarrow \forall x\in\partial\Omega\cap D\\ &\Phi(x) < 0 \Longleftrightarrow \forall x\in\Omega\\ &\Phi(x) > 0 \Longleftrightarrow \forall x\in(D\backslash\overline{\Omega})\end{aligned}$$

where D is a fixed domain in which all admissible shapes Ω are included, i.e. $\Omega\subset D$. In the level set method, the scalar function Φ can be specified in any specific form, and it is often described in a discrete counterpart. In most cases Φ is specified by a regular sampling on a rectilinear grid and constructed to be a signed distance function to the boundary. With such a signed distance function ($|\nabla\Phi|\equiv 1$), many geometric properties of the boundary can be readily expressed, for instance the unit outward normal n of the boundary is given by $n = \nabla\Phi$.

Propagation of the Neumann boundary of a structure during the course of optimization is described by the Hamilton–Jacobi equation:

$$\frac{\partial\Phi}{\partial t} + V_n = 0 \tag{21}$$

The design velocity V_n is an important link between the level set method and an optimization algorithm [25]. During the course of optimization, variation of boundary shape that improves the current design is obtained as a result of shape sensitivity analysis. The boundary variation is then treated as an advection velocity in the Hamilton–Jacobi equation for updating the boundary of a structure. In other words, an optimization algorithm gives the desired variation of the free boundary, while the Hamilton–Jacobi equation performs the variation. The level set based shape and topology optimization method is a boundary variation method that essentially maintains the 0–1 nature of topology optimization [37].

An important property of the Hamilton–Jacobi equation Eq. (21) is that it satisfies the maximum principle, and as a result voids can not be nucleated in the interior of a structure [24]. This makes the level set based topology optimization, especially in 2D, be sensitive to initial design [24]. To overcome this dependence much effort has been made to incorporate the topological derivative [38] into the level set based method [39–41]. The situation is slightly different in 3D in that although a new void cannot be nucleated right in the interior of a structure, a hole can be "tunneled" through the material region in between two pieces of boundary [42]. Therefore, as compared to the situation in 2D, the level set based optimization in 3D is topologically more flexible and less sensitive to the initial design. In our present study we use the conventional level set method without using the topological derivative.

It should be noted that in the level set based method the design velocity V_n defined on the traction free Γ_H must be extended to the entire reference domain D or a narrow band around Γ_H [43,44]. Conventionally, in the level set based method for topology optimization, a fixed mesh is used for the finite element analysis, and voids ($D\backslash\overline{\Omega}$) are mimicked by artificial weak material,therefore the design velocity can be naturally extended to the entire reference domain D as $V_n^e = V_n, \forall x\in D$. In the present work, however, since we do not use artificial weak material but modify a fixed background mesh for the finite element analysis, the above-mentioned natural extension of velocity is no longer valid. Therefore, the PDE based method for velocity extension [45] is used in the present study.

The Hamilton–Jacobi equation Eq. (21) is a hyperbolic type of PDE [43,44]. A variety of spatial and time discretization schemes were devised to solve this type of PDE. In the present study, the first order upwind spatial differencing and forward Euler time differencing are utilized. Finally, since the level set function Φ often

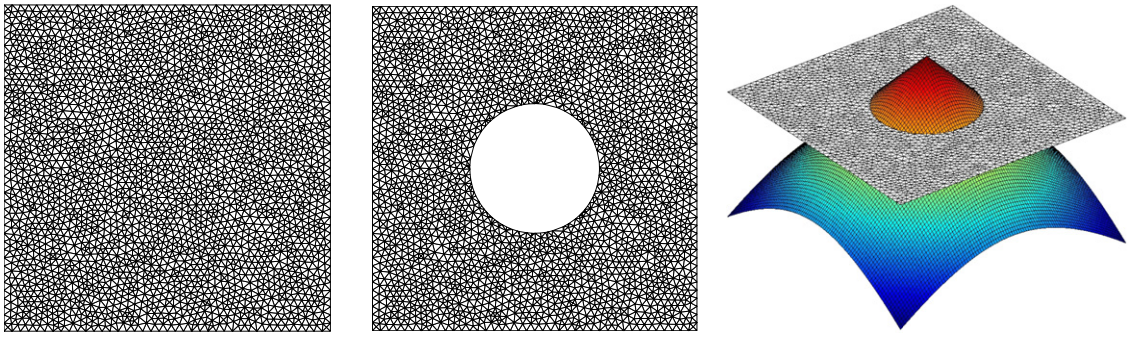

(a) background mesh (b) final mesh (c) background mesh and Φ

Fig. 2. An example of the modification of a background mesh.

becomes too flat or too steep during the optimization that leads to accumulating numerical errors, a reinitialization procedure is periodically performed to restore Φ to a signed distance function to the traction free boundary, i.e., to restore $|\nabla\Phi| = 1$. More details of the numerical computations of level set can be found in [43,44].

5. Finite element analysis

Conventionally, an Eulerian method employing a fixed mesh and ersatz material is used for the finite element analysis in the level set based method of topology optimization. In this method, instead of solving the linear elasticity system on Ω, one solves it on the entire reference domain D with the void $D\backslash\overline{\Omega}$ being mimicked by an artificial weak material. The material properties of the artificial weak material are tailored so that the results of the finite element analysis obtained on the entire reference domain D be consistent to that which would be obtained on Ω. However, in the present study of stress-based topology optimization of continuum structures, the Eulerian method is not accurate enough, and we choose to do the finite element analysis by modifying a fixed background mesh and do not use artificial weak material. The reason for choosing such a FEA method is twofold and was explained in Section 1.

Before the optimization, we setup a background triangle mesh for the reference domain D. In each iteration of the optimization, modification of the fixed background mesh is performed to obtain a mesh that is conformal to the geometry of the structure. The modification is divided into several steps.

1. Find the edges of the background mesh that are cut by the free boundary of the structure. Then, compute all the intersecting points and obtain a point set P_0.
2. Find the nodal points of the background mesh that are within the region of the structure Ω and obtain a point set P_1.
3. Setup a point set P that comprises P_0 and P_1, and triangulate the points of the set P using the Delaunay triangulation algorithm.
4. Delete the triangles whose centroid are out of Ω or out of D, and delete unused node points.
5. Adjusting the node point positions of the mesh to obtain better quality of mesh.

A simple example of the modification of the background mesh is shown in Fig. 2. If one amplifies Fig. 2(b), one can see that the circular boundary of the structure is actually represented by many line segments, and that the slope of these line segments are not continuous. This may lead to weak stress singularity at the points of slope discontinuity. Such situation is well-known in shape optimization. In the early studies of shape optimization, position of the nodes of finite element mesh were taken as the design variables [1,2], but such approach gives rise to zigzag boundary as described by Braibant and Fleury [46], hence they proposed to use smooth parameterized curve, for instance the B-splines, to represent the boundary. Various techniques of boundary parametrization for shape optimization were reviewed by Haftka and Grandhi [47] and by Ding [3]. In our present work, there indeed exists discontinuity of slope along the boundary, but it will not result in zig–zag boundary, because that the numerical viscocity in the solution of the Hamilton–Jacobi equation damps kinks along the boundary [48].

Using the above-mentioned FEA method in topology optimization, floating regions in the reference domain may arise during the optimization. One needs to be careful with such floating regions when solving the adjoint equation Eq. (16), because the von Mises stress in such regions is zero and leads to zero denominator in Eq. (13). Such floating regions are not considered when solving the adjoint equation.

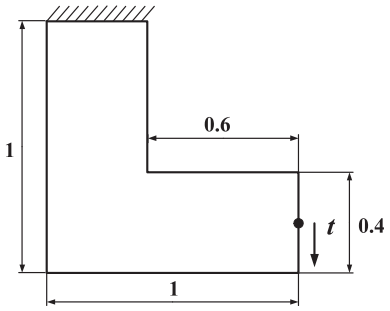

Fig. 3. Design problem of a L-shape beam.

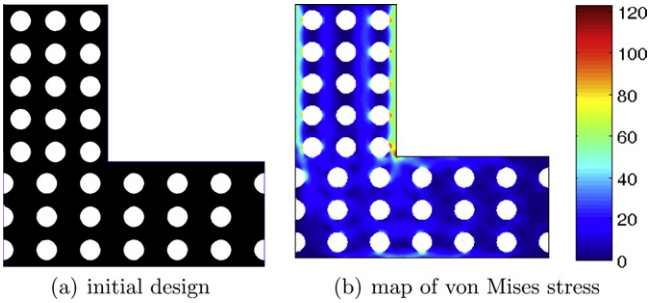

(a) initial design (b) map of von Mises stress

Fig. 4. Initial design of the L-shape beam and map of the von Mises stress.

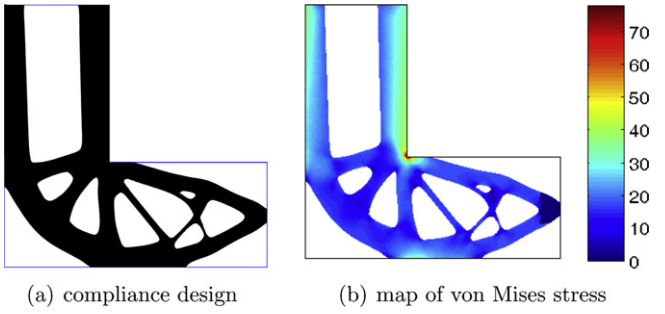

Fig. 5. Results of compliance optimization.

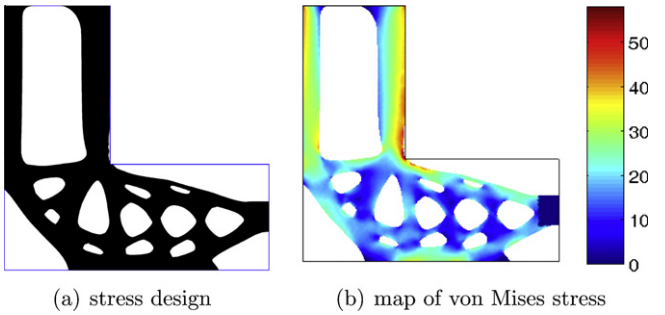

Fig. 6. Results of stress optimization ($\alpha_1 = 1, \alpha_2 = 10, p = 2, \bar{\sigma} = 55, \Delta = 5$).

6. Numerical examples

In this section the proposed level set based method is applied to several examples in two dimensions, although there exists no conceptual difficulty to do the numerical examples in three dimensions. In these examples, it is assumed that the solid material has a Young's modulus $E = 1$ and Poisson's ratio $\nu = 0.3$. For all the examples, the plane stress state is assumed, and linear triangle finite element is used. Moreover, the high stresses in the vicinity around the point where a support or a concentrated load is applied are not considered in the global measure of stress.

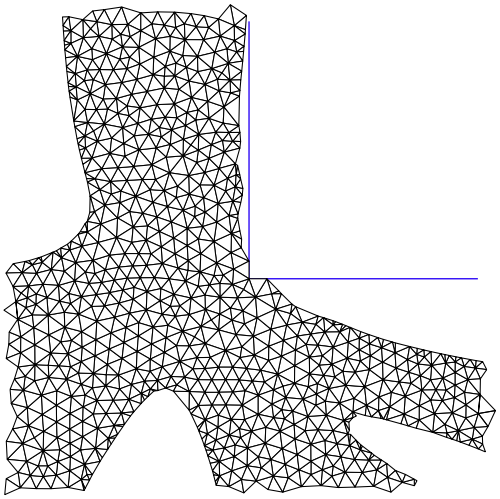

Fig. 8. Finite element mesh around the inner corner of the stress design.

6.1. A L-shape beam

The optimal design problem of a *L*-shape beam is shown in Fig. 3. A unit vertical concentrated load $t = 1$ N is applied at the middle point of the right side. The initial design and the map of von Mises stress are shown in Fig. 4. Note that in all the stress plot, the stresses in the vicinity around the point where a concentrated

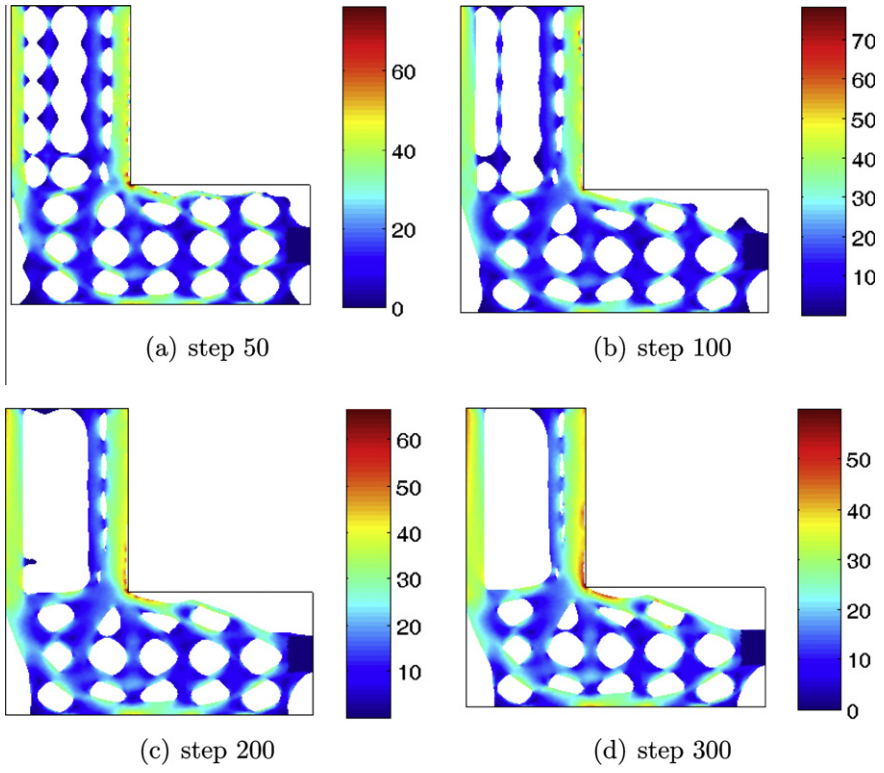

Fig. 7. Intermediate results of stress optimization.

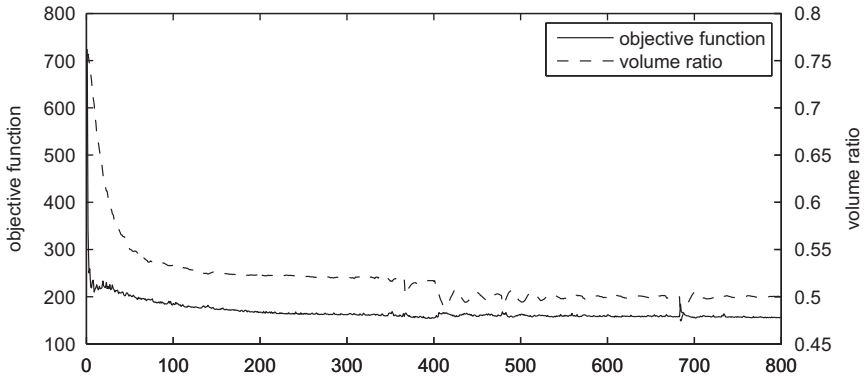

Fig. 9. Convergence history of stress minimization.

load is applied is artificially set to zero. There are 21979 linear triangle elements in the background mesh for the *L*-shaped reference domain.

First, to provide a reference for the stress-based topology optimization, a compliance-based topology optimization is solved. In this optimization, the compliance is minimized subject to a volume constraint that the volume of material should not be bigger than 50% of the reference domain. The results are shown in Fig. 5, and one can see that there is stress concentration at the inner corner of the compliance design. The maximal von Mises stress is more than 70.

Second, the proposed global measure of von Mises stress, with the parameters being set as $\alpha_1 = 1, \alpha_2 = 10, p = 2, \bar{\sigma} = 55, \Delta = 5$, is minimized subject to the same volume constraint. The results are shown in Fig. 6. The maximal von Mises stress is 58. Comparing the stress design and compliance design, one can see that the two designs are quite different, particularly at the inner corner. The intermediate results of optimization are shown in Fig. 7. The finite element mesh around the inner corner is shown in Fig. 8. Finally, the convergence history is shown in Fig. 9, and one can see that the convergence is smooth.

In the proposed global measure of von Mises stress, there are five parameters, i.e., $\alpha_1, \alpha_2, p, \bar{\sigma}$, and Δ that need to be specified before optimization and have significant effects on the results. First, if $\alpha_2 = 0$, the global measure is just $\int_\Omega \sigma_v^p \, dx$ which is similar to the *p*-norm or *p*-mean, and big *p* is needed to control the peak stress at the inner corner (for instance, readers are referred to the numerical examples in [9,14]). Second, if $\alpha_1 = 0$ and Δ is not too big, for example $\alpha_1 = 0, \alpha_2 = 1, p = 2, \bar{\sigma} = 55, \Delta = 5$, the measure $\int_\Omega \sigma_v^2 H(\sigma_v - 55) \, dx$ is actually not a global measure, since it considers only the von Mises stress that is bigger than $\bar{\sigma} - \Delta = 50$. In this case, during the optimization the boundary around the inner corner is smoothed but the other parts of the free boundary are not optimized properly. Third, the parameter $\bar{\sigma}$ is a threshold of von Mises stress, and the penalty of stress is gradually increase from 0 for $\sigma_v \leqslant \bar{\sigma} - \Delta$ to α_2 for $\sigma_v \geqslant \bar{\sigma} + \Delta$. According to our experience, $\bar{\sigma}$ should not be too small for obtaining effective control over the peak stress. In an extreme case that $\bar{\sigma} = 0$, the global measure is

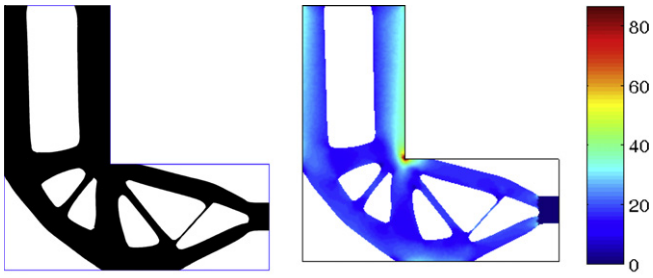

Fig. 10. Results of stress optimization ($\alpha_1 = 1$, $\alpha_2 = 0$, $p = 2$).

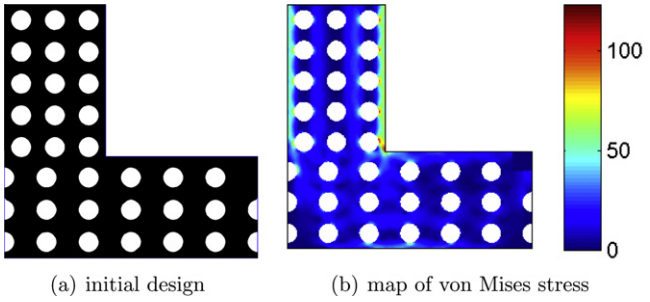

Fig. 12. Initial design of another *L*-shape beam and map of the von Mises stress.

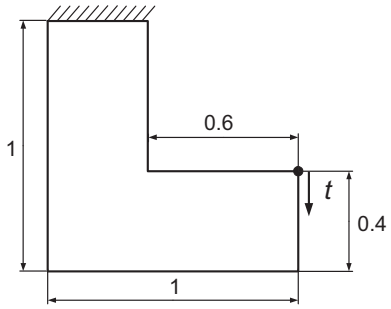

Fig. 11. Design problem of another *L*-shape beam.

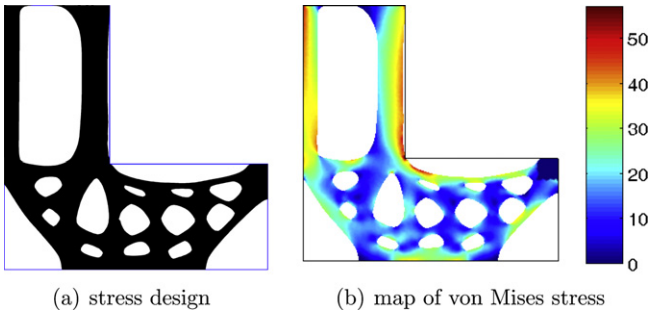

Fig. 13. Results of stress optimization ($\alpha_1 = 1, \alpha_2 = 20, p = 2, \bar{\sigma} = 55, \Delta = 5$).

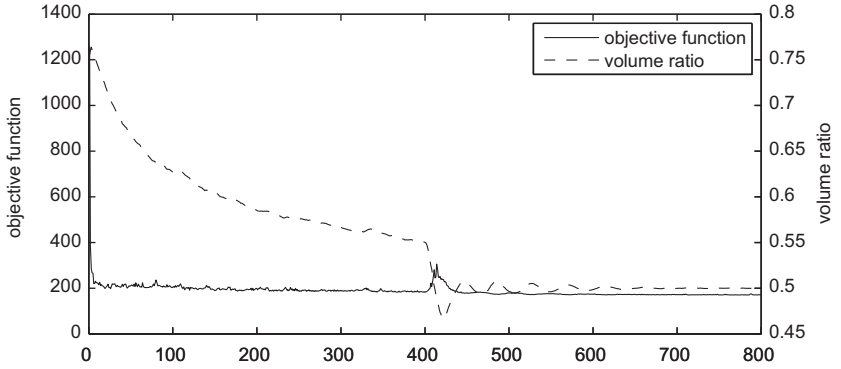

Fig. 14. Convergence history of stress minimization.

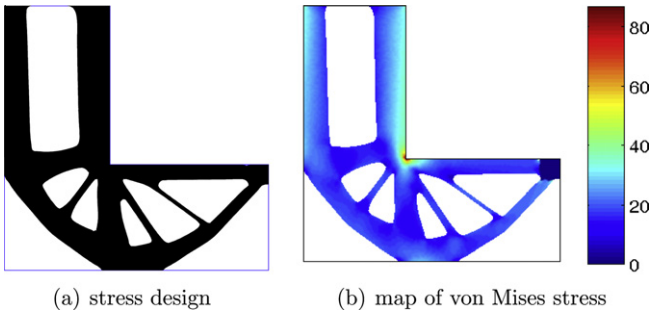

Fig. 15. Results of stress optimization ($\alpha_1 = 1$, $\alpha_2 = 0$, $p = 2$).

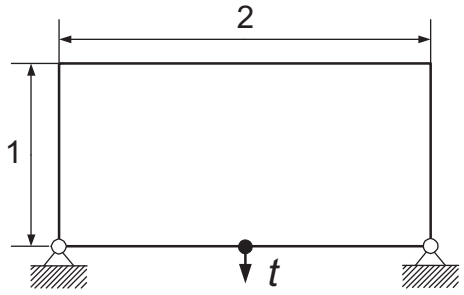

Fig. 16. Design problem of a Michell structure.

nearly equivalent to the p-norm, and it cannot effectively control the peak stress. Finally, the parameter Δ controls the width of transition band of the Heaviside function, and it affects the smoothness of the convergence of the stress-based optimization. When Δ is too small, the convergence becomes oscillatory, due to the abrupt change of penalty of stress from point to another point in the structure. In other word, if the parameter Δ is sufficiently large, one obtains a penalty that changes smoothly in a neighborhood around a point of peak stress. However, Δ should not be too big, otherwise the global measure will be nearly equivalent to the p-norm, and it cannot effectively control the peak stress. To conclude, the five parameters give flexible control of the peak stress and the convergence of optimization. The drawback is that the value of the five parameters needs to be specified by the designer and cannot be automatically adapted during the optimization. In particular, if $\bar{\sigma}$ can be gradually reduced during the optimization, it will be useful for stress constrained optimization.

In order to verify the effect of the penalty term in the global measure, the proposed global measure with the parameters being set as $\alpha_1 = 1$, $\alpha_2 = 0$, $p = 2$, i.e., $\int_\Omega \sigma_v^2 dx$, is minimized subject to the same volume constraint. The results are shown in Fig. 10. As we can see, there is stress concentration at the inner corner. The maximal von Mises stress is 86. Therefore, without the penalty term the global measure with a small $p = 2$ is not able to control the peak stress.

In the literature, another design problem of the L-shaped beam, shown in Fig. 11 is also often considered. In this design problem, the concentrated load is applied at the tip of the right side of the beam. The initial design and the map of von Mises stress are shown in Fig. 12. Note that in all the stress plot, the stresses in the vicinity around the point where the concentrated load is applied is artificially set to zero. The maximal von Mises stress of the initial design is 123. The proposed global measure of von Mises stress, with the parameters being set as $\alpha_1 = 1, \alpha_2 = 20, p = 2, \bar{\sigma} = 55, \Delta = 5$, is minimized subject to a volume constraint that the volume of material should not be bigger than 50% of the reference domain. The results are shown in Fig. 13. The maximal von Mises stress is 57. One can see that the boundary at the inner corner is smooth. The convergence history is shown in Fig. 14. In order to verify the effect of the penalty term in the global measure, the proposed global measure with the parameters being set as $\alpha_1 = 1$, $\alpha_2 = 0$, $p = 2$, i.e., $\int_\Omega \sigma_v^2 dx$, is minimized subject to the same volume constraint. The results are shown in Fig. 15. As we can see, there is stress concentration at the inner corner. The maximal von Mises stress is 87.

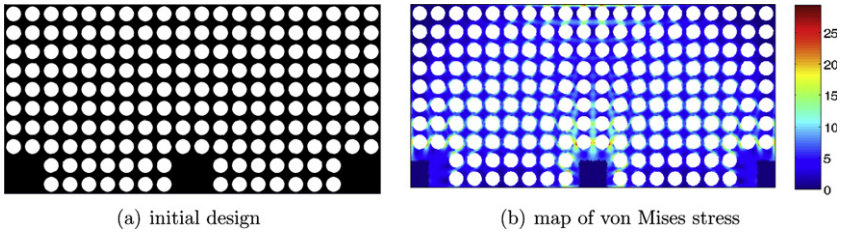

Fig. 17. Initial design of a Michell structure and map of the von Mises stress.

Therefore, without the penalty term the global measure with a small $p = 2$ is not able to control the peak stress.

6.2. A Michell structure

The optimal design problem of a Michell structure is shown in Fig. 16. A unit vertical point load $t = 1$ N is applied at the middle point of the bottom side. The initial design and the map of von Mises stress are shown in Fig. 17. Note that in all the stress plot, the stresses in the vicinity around the point where a concentrated load is applied and around the support is artificially set to zero. Due to the symmetry of the boundary and loading conditions, the finite element analysis is done for only a half of the reference domain. There are 17216 linear triangle elements in the background mesh for a half of the design domain.

The proposed global measure of von Mises stress, with the parameters being set as $\alpha_1 = 1, \alpha_2 = 10, p = 2, \bar{\sigma} = 10, \Delta = 5$, is minimized subject to a volume constraint that the volume of material should not be bigger than 30% of the reference domain. The results are shown in Fig. 18. The maximal von Mises stress is 9. The convergence history is shown in Fig. 19. Moreover, to provide a reference for the stress-based topology optimization, a compliance-based topology optimization is solved. In this optimization, the compliance is minimized subject to the same volume constraint. The results are shown in Fig. 20. The maximal von Mises stress is 9.

One can see that for the Michell structure, the stress design and the compliance design are almost the same. It was shown by Pedersen [49] that the stiffness design is also the strongest design so long as geometric constraint is not active. In fact, in the numerical example of the *L*-shape beam, the reference domain *D* is indeed a geometric constraint, since the free boundary of the optimal stiffness design or the compliance design adjoint the boundary of the reference domain. Therefore, for the *L*-shape example, the stiffness design is quite different from the strongest design or the stress design. As for the current example of the Michell structure, the free boundary of both the compliance design and stress design do not adjoint the boundary of the reference domain, and the two designs are almost the same.

Besides the above-mentioned geometric constraint, there also exist other important reasons for the differences between the resulting designs of a stress-based optimization and a compliance-based optimization. Duysinx et al. [50] demonstrated by numerical examples that when stress limits are unequal in tension and compression or when multiple load cases are considered, the results of a compliance-based optimization and a stress-based optimization may be quite different. Therefore, the authors [50] pointed out that it

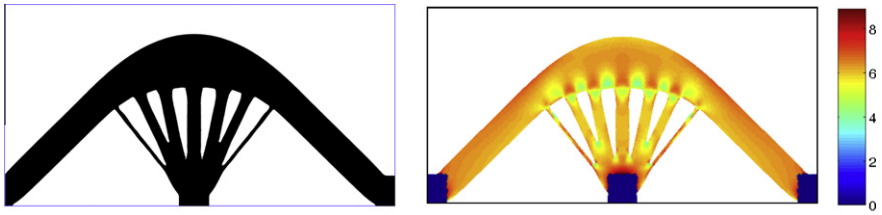

(a) stress design (b) map of von Mises stress

Fig. 18. Results of stress optimization ($\alpha_1 = 1, \alpha_2 = 10, p = 2, \bar{\sigma} = 10, \Delta = 5$).

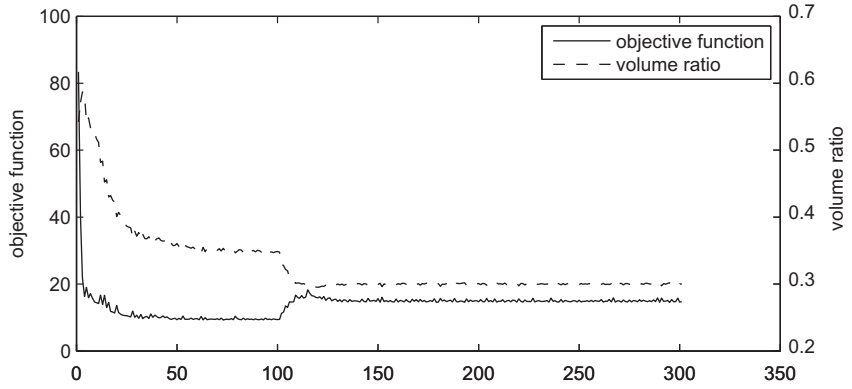

Fig. 19. Convergence history of stress minimization.

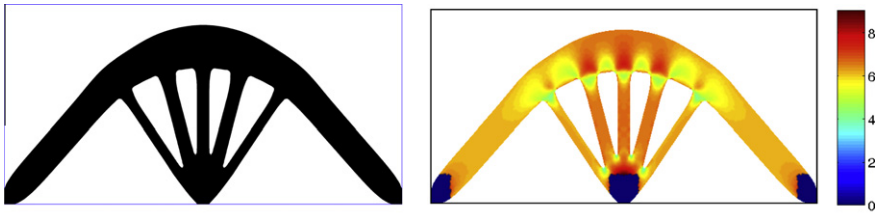

(a) compliance design (b) map of von Mises stress

Fig. 20. Results of compliance optimization.

is important to consider stress as early as possible in the design process, for example considering stress in the phase of the topology optimization based concept design.

7. Conclusion

In this paper, we presented a level set solution to the stress-based shape and topology optimization. A novel global measure of stress is proposed for the stress-based structural shape and topology optimization. The level set method is employed to solve the optimization problem. The shape sensitivity analysis is performed via the material derivative method. The finite element analysis is accomplished by modifying a fixed background mesh, and the artificial weak material that is conventionally used in the level set method to mimic void is avoided in the present work. Application of the method is demonstrated by several numerical examples of 2D structures. As we can see, the peak stress can be effectively controlled during the optimization and the convergence of the optimization is smooth.

Acknowledgements

This research work is partly supported by the Fundamental Research Funds for the Central Universities, HUST, (Grant No. Q2009009, 2011QN033), the Natural Science Foundation of Hubei province (Grant No. 2009CDB321), and the National Natural Science Foundation of China (Grant No. 51075161), which the authors gratefully acknowledge. The insightful comments of the reviewers' are cordially appreciated.

References

[1] Zienkiewicz OC, Campbell JS. Shape optimization and sequential linear programming. In: Gallagher RH, Zienkiewicz OC, editors. Optimum structural design: theory and applications. Wiley; 1973. p. 109–26.
[2] Francavilla A, Ramakrishnan CV, Zienkiewicz OC. Optimization of shape to minimize stress concentration. J Strain Anal 1975;10:63–70.
[3] Ding Y. Shape optimization of structures: a literature survey. Comput Struct 1986;24:984–1004.
[4] Meske R, Sauter J, Schnack E. Nonparametric gradient-less shape optimization for real-world applications. Struct Multidiscip Optim 2005;30:201–18.
[5] Bendsøe MP, Kikuchi N. Generating optimal topologies in structural design using a homogenization method. Comput Methods Appl Mech Eng 1988;71:197–224.
[6] Bendsøe MP. Optimal shape design as a material distribution problem. Struct Optim 1989;1:193–202.
[7] Yang RJ, Chen CJ. Stress-based topology optimization. Struct Optim 1996;12:98–105.
[8] Duysinx P, Bendsøe MP. Topology optimization of continuum structures with local stress constraints. Int J Numer Methods Eng 1998;43:1453–78.
[9] Allaire G, Jouve F, Maillot H. Topology optimization for minimum stress design with the homogenization method. Struct Multidiscip Optim 2004;28:87–98.
[10] Pereira JT, Fancello EA, Barcellos CS. Topology optimization of continuum structures with material failure constraints. Struct Multidiscip Optim 2004;26:50–66.
[11] Bruggi M, Venini P. A mixed FEM approach to stress-constrained topology optimization. Int J Numer Methods Eng 2008;73:1693–714.
[12] París J, Navarrina F, Colominas I, Casteleiro M. Topology optimization of continuum structures with local and global stress constraints. Struct Multidiscip Optim 2009;39:419–37.
[13] París J, Navarrina F, Colominas I, Casteleiro M. Stress constraints sensitivity analysis in structural topology optimization. Comput Methods Appl Mech Eng 2010;199:2110–22.
[14] Le C, Norato J, Bruns T, Ha C, Tortorelli D. Stress-based topology optimization for continua. Struct Multidiscip Optim 2010;41:605–20.
[15] Svanberg K, Werme M. Sequential integer programming methods for stress constrained topology optimization. Struct Multidiscip Optim 2007;34: 277C299.
[16] Li Q, Steven GP, Xie YM. Evolutionary thickness design with stiffness maximization and stress minimization criteria. Int J Numer Methods Eng 2001;52:979–95.
[17] Amstutz S, Novotny AA. Topological optimization of structures subject to von mises stress constraints. Struct Multidiscip Optim 2010;41:407–20.
[18] Allaire G, Jouve F. Minimum stress optimal design with the level set method. Eng Anal Bound Elem 2008;32:909–18.
[19] Miegroet LV, Duysinx P. Stress concentration minimization of 2D filets using X-FEM and level set description. Struct Multidiscip Optim 2007;33:425–38.
[20] Poon NMK, Martins JRRA. An adaptive approach to constraint aggregation using adjoint sensitivity analysis. Struct Multidiscip Optim 2007;34:61–73.
[21] Sethian JA, Wiegmann A. Structural boundary design via level set and immersed interface methods. J Comput Phys 2000;163:489–528.
[22] Osher S, Santosa F. Level-set methods for optimization problems involving geometry and constraints: frequencies of a two-density inhomogeneous drum. J Comput Phys 2001;171:272–88.
[23] Allaire G, Jouve F, Toader AM. A level-set method for shape optimization. CR Acad Sci Paris Ser I 2002;334:1–6.
[24] Allaire G, Jouve F, Toader AM. Structural optimization using sensitivity analysis and a level-set method. J Comput Phys 2004;194:363–93.
[25] Wang MY, Wang XM, Guo DM. A level set method for structural topology optimization. Comput Methods Appl Mech Eng 2003;192:227–46.
[26] Kirsch U. On singular topologies in optimum structural design. Comput Methods Appl Mech Eng 1990;2:133–42.
[27] Cheng GD, Jiang Z. Study on topology optimization with stress constraints. Eng Optim 1992;20:129–48.
[28] Rozvany GIN, Birker T. On singular topologies in exact layout optimization. Struct Optim 1994;8:228–35.
[29] Rozvany GIN. On design-dependent constraints and singular topologies. Struct Multidiscip Optim 2001;21:164–72.
[30] Cheng GD, Guo X. ε-relaxed approach in structural topology optimization. Struct Optim 1997;13:258–66.
[31] Bruggi M. On an alternative approach to stress constraints relaxation in topology optimization. Struct Multidiscip Optim 2008;36:125–41.
[32] Choi KK, Kim NH. Structural sensitivity analysis and optimization. Springer; 2005.
[33] Haug EJ, Choi KK, Komkov V. Design sensitivity analysis of structural systems. Academic Press; 1986.
[34] Nocedal J, Wright SJ. Numerical optimization. Springer; 1999.
[35] Wang XM, Wang MY, Guo DM. Structural shape and topology optimization in a level-set framework of region representation. Struct Multidiscip Optim 2004;27:1–19.
[36] Mei Y, Wang X. A level set method for structural topology optimization and its applications. Adv Eng Softw 2004;35:415–41.
[37] Xia Q, Wang MY. Topology optimization of thermoelastic structures using level set method. Comput Mech 2008;42:837–57.
[38] Sokolowski J, Zochowski A. On the topological derivative in shape optimization. SIAM J Control Optim 1999;37:1251–72.
[39] Allaire G, Jouve F. Coupling the level set method and the topological gradient in structural optimization. In: Bendsøe MP, Olhoff N, Sigmund O, (Eds.). Topological design optimization of structures, machines and materials, vol. 137, 2006. p. 3–12.
[40] Burger M, Hackl B, Ring W. Incorporating topological derivatives into level set methods. J Comput Phys 2004;194:344–62.
[41] He L, Kao C, Osher S. Incorporating topological derivatives into shape derivative based level set methods. J Comput Phys 2007;225:891–909.
[42] Xia Q, Shi TL, Wang MY, Liu SY. A level set based method for the optimization of cast part. Struct Multidiscip Optim 2010;41:735–47.
[43] Sethian JA. Level set methods and fast marching methods: evolving interfaces in computational geometry, fluid mechanics, computer vision, and materials science, cambridge monographs on applied and computational mathematics. 2nd ed. Cambridge, UK: Cambridge University Press; 1999.
[44] Osher S, Fedkiw R. Level set methods and dynamic implicit surfaces. New York: Springer-Verlag; 2002.
[45] Peng DP, Merriman B, Osher S, Zhao HK, Kang M. A PDE-based fast local level set method. J Comput Phys 1999;155:410–38.
[46] Braibant V, Fleury C. Shape optimal design using *B*-splines. Comput Methods Appl Mech Eng 1984;44:247–67.
[47] Haftka RT, Grandhi RV. Structural shape optimization—a survey. Comput Methods Appl Mech Eng 1986;57:517–22.
[48] Osher S, Fedkiw R. Level set methods: an overview and some recent results. J Comput Phys 2001;169:463–502.
[49] Pedersen P. On optimal shapes in materials and structures. Struct Multidiscip Optim 2000;19:169–82.
[50] Duysinx P, Miegroet LV, Lemaire E, Bruls O, Bruyneel M. Topology and generalized shape optimization: why stress constraints are so important? Int J Simul Multidiscip Des Optim 2008;2:253–8.